JET–R(97)03

Deuterium Implantation in Actively Cooled Beryllium Monoblocks

H D Falter, D Ciric, J P Coad, D Godden.

JET Joint Undertaking, Abingdon, Oxfordshire, OX14 3EA, UK.

April 1997

1. INTRODUCTION

The amount of tritium buried in the first wall of a fusion reactor could turn out to be the decisive factor for the choice of wall material. In the case of copper, the common material for beam dumps, we have found a large discrepancy between data published from surface analysis groups and data from neutron generators on the amount of implanted hydrogen [1]. In neutron generators with high particle energies and fluxes, trapping appears to be dominant and implanted hydrogen concentrations of up to 40 at% are reported [2,3]. Well controlled low flux experiments done for surface analysis yield concentrations below 1 at% and the amount of implanted hydrogen is dominated by diffusion and surface recombination [4]. To investigate if similar discrepancies are found in Beryllium we analysed a test section with Nuclear Reaction Analysis after an exposure test with Deuterium beams. In this exposure surface temperature and power density are representative of a first wall component. However the particle energy is higher than for first wall components and the flux is correspondingly lower.

The test section is an actively cooled Beryllium Monoblock (Brush Wellman grade S65C) which had been used before for several power handling tests. Part of the surface had been above liquidus in these tests with a melt depth of less than 1 mm. Aim of this experiment was to determine the quantity if implanted deuterium with Nuclear Reaction Analysis. The experiment was done in two steps:

1. The test section was exposed to a power density of 4 - 5 MW/m^2 and analysed some days after exposure.
2. The test section was exposed to high power densities of 20 MW/m^2 which brings the surface into melting and was analysed after exposure.

2. EXPERIMENTAL SETUP

Fluxes, energies and temperatures of this section refer to the first part of the experiment in which the surface temperature of the beryllium was well below melting.

The experimental setup is the same as in the previous experiment [5]: The test section consists of 20 Beryllium monoblocks brazed onto a 12 mm id cooling pipe (Fig.1). A disc assembly consisting of two silicon wafers and one glass disc was installed above the test section at a distance of approximately 230 mm measured along the line connecting the centers of test section and disc holder. This line is at

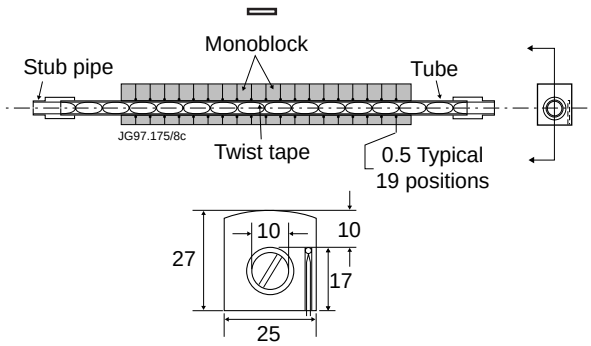

Fig.1: Schematic of the test section: Beryllium monoblocks are brazed to copper cooling pipe. The full length of the test section is exposed.

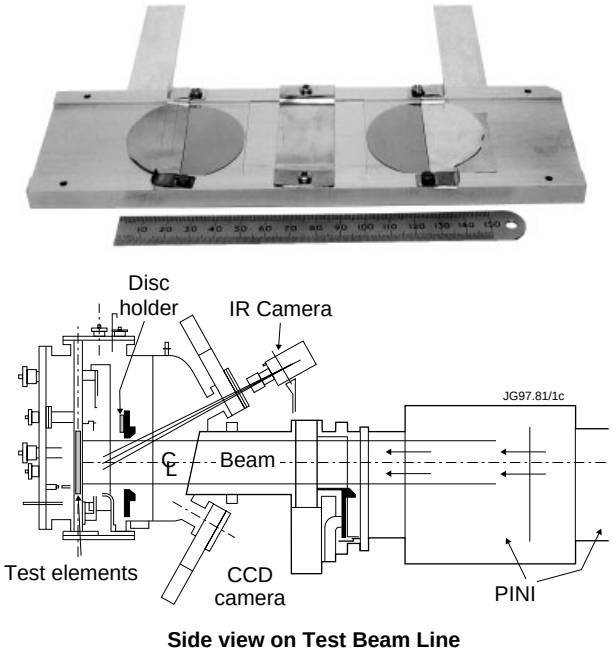

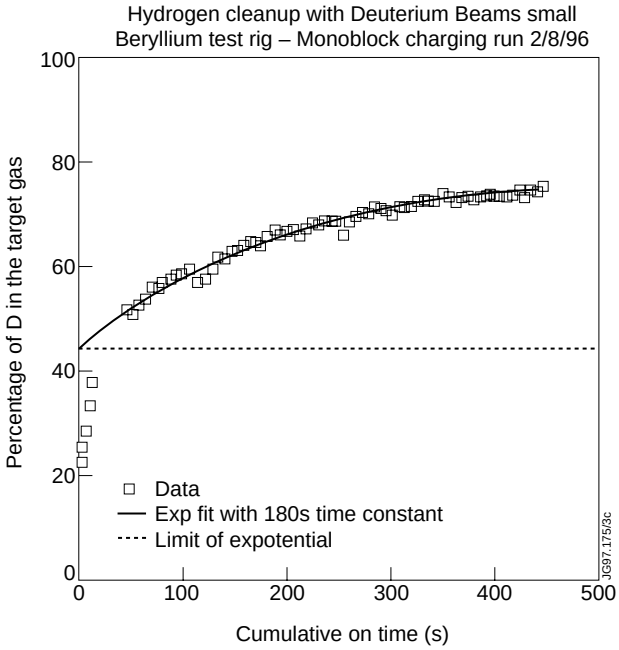

Fig.2: Elevation of the test section. A disk holder is mounted vertically behind the top scraper at 230 mm from the test section.

Fig.3: Deuterium content in the beam. The gas used for the beam is partially recycled and the hydrogen is only gradually replaced by deuterium.

an angle of 45 degree to the surface of the test section (Fig.2). A photograph of the disc assembly is inserted in Fig.2

The test section was exposed to a composite beam of Hydrogen and Deuterium ions and neutrals accelerated to 60 keV. The deuterium content in the beam increased steadily from initially 20% to 75% at the end of the panel charging. Deuterium content and beam composition where measured by H_α spectroscopy. The composition of Hydrogen and Deuterium is derived from the unshifted peaks and shown in Fig.3, the species mix of the deuterium part of the beam is given in table 1:

Table 1: Composition of the deuterium fraction (ions and neutrals) during charging				
Component	Full energy	Half energy	Third energy	Impurities
Composition (% of power)	43.4	10.5	34	12
Commposition (% of flux)	22	10	50	18
Energy per atom [keV]	60	30	20	3.2

Fig.4 shows a plan view of the experimental setup. The test section is partially shaded by a scraper. The inertial calorimeter is behind the test section.

The upper part of the test section can not be seen by the IR imaging system (Fig.2) and no measurement of the surface temperature is available for this upper part. By comparing the

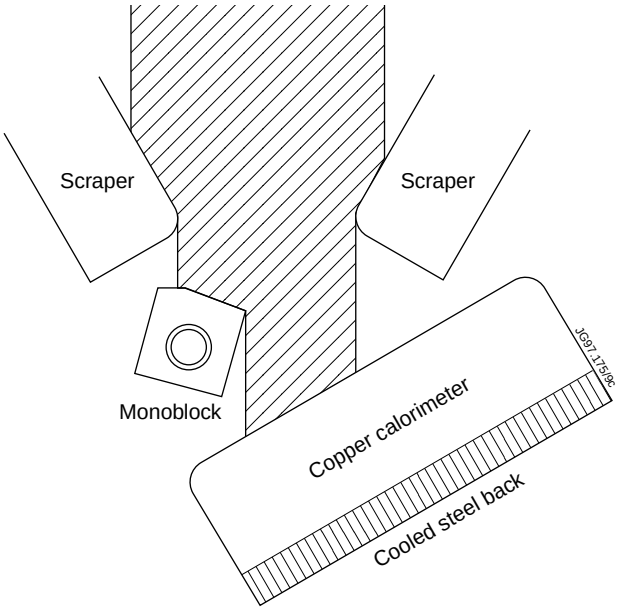

Fig.4: Plan view of the test setup. The monoblock is partially shaded by a scraper. The calorimeter is mounted behind the test section.

vertical profiles from the surface temperature (IR), the bulk temperature (TC) and the power density (inertial calorimeter) (Fig.5 and Fig.6) we can see that all three quantities are proportional to each other. This allows estimate a surface temperature from the bulk temperature by using the correlation $T_{surface} = 2.15 \times T_{bulk}$ (temperature in ^{o}C).

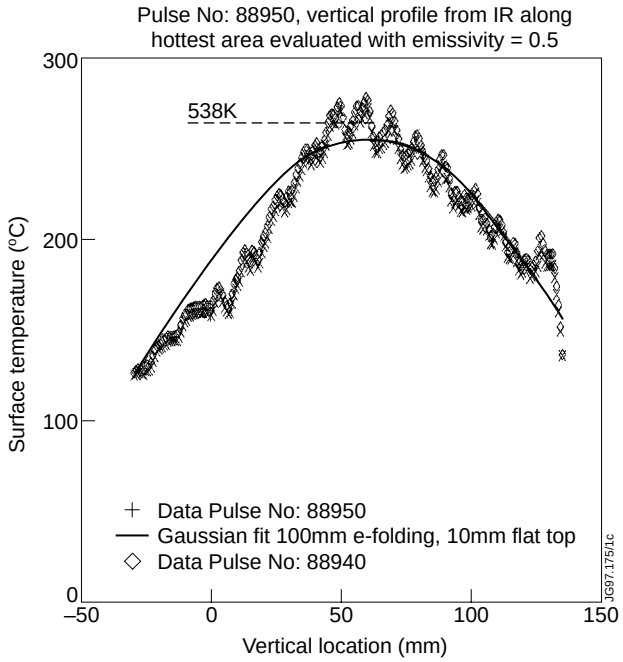

Fig.5: Vertical profile of the surface temperature along a line through the hottest parts. Surface temperature and bulk temperature (10 mm below the exposed surface) have the same profile.

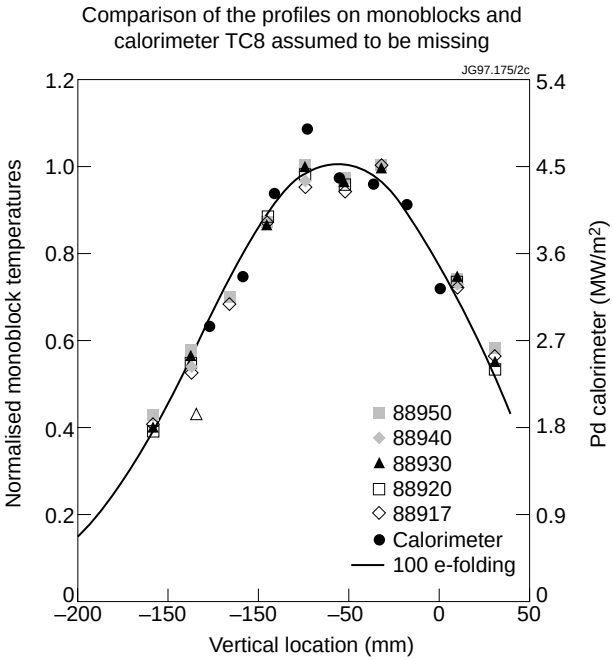

Fig.6: Vertical profile of the bulk temperature (10 mm below the exposed surface) and of the power density from the inertial calorimeter. The profiles are identical.

The time constants for the exponential temperature rise during exposure and the cooldown after exposure are 2.6 seconds for the heat up and 1 second for the cooldown (Fig.7). The test section was exposed to 6 s pulses with a typical duty cycle of 15 pulses per hour. The water cooling loop was at room temperature. The test section was exposed to a peak fluence of 2 10^{19} deuterium atoms/cm^2 during 450 s of exposure (Fig.8).

The main parameters of the first part of the experiment are shown in annex 1.

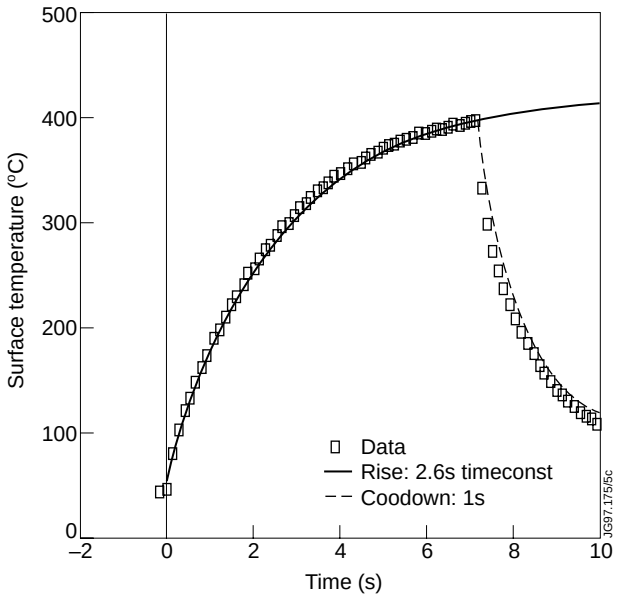

Fig.7: Time constants of the surface temperature.

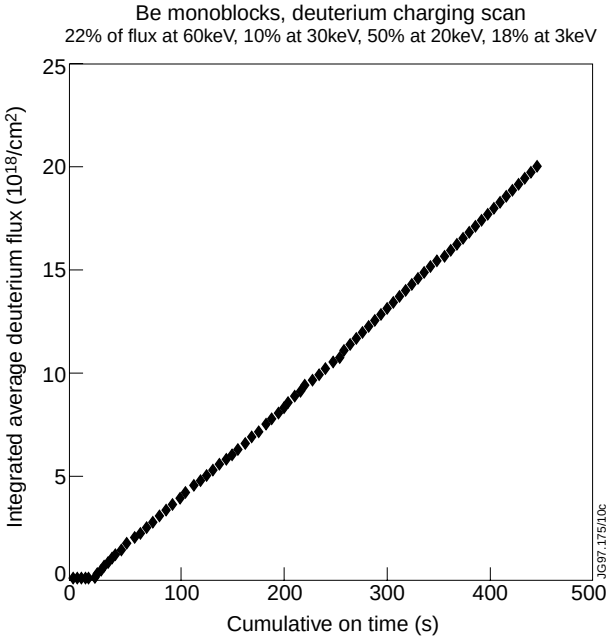

Fig.8: Fluence versus exposure time. The total fluence was 2.2 10^{19} atoms/cm^2.

2.1 Concentration measurement

After charging the test section was exposed to air for 6 days before the concentration was measured with Nuclear Reaction Analysis. The Monoblock was mounted in aspecial large vacuum chamber with Be-handling facilities attached to the University of Sussex 3 MeV accelerator. For D analysis a 2.5 MeV 3He beam was used, and protons produced by the reaction

$$D(^3He, p)^4He$$

Simultaneously Be and C can be measured using the reactions

$$^9Be(^3He, p)^{11}B, \quad ^{12}C(^3He, p)^{14}N$$

The exact energy of the proton peak from the reaction with D depends on the depth within the surface from which the proton was emitted, so that the peak shape gives a picture of the distribution of D within the surface: the maximum depth from which information can be derived with a 2.5 MeV beam is 8 μm.

3. EXPERIMENTAL RESULTS.

3.1 Implanted concentration

Table 2 shows the measured concentration for tiles 1, 3, 5, 7, 9, and 11, measured in the center of the tiles, and the typical bulk temperature rise of the respective tile, measured with a thermocouple 10 mm below the exposed surface. The tile numbering is from top to bottom.

Table 2: Tc temperature and deuterium concentration

	run without surface melting		run with surface melting	
block	concentration $10^{18}/cm^2$	temperature (°C)[1]	concentration $10^{18}/cm^2$	temperature (°C)[2]
1	1.7	51 (383)	0.36	169 (1070)
2			0.13	(1270)
3	1.74	69 (421)	0.009	244 (1470)
5	1.63	86 (458)	0	320
7	1.51	109 (508)	00	400
9	1.66	120 (531)	0	449
11	1.67	121 (533)	0	443

[1] This is the peak TC temperature measured 10 mm below the exposed surface. In brackets the estimated surface temperature is given in ^oK

[2] In brackets given is a rough estimate of the surface temperature as explained in the text.

The measured concentrations after the charging run at 5 MW/m^2 are almost uniform. Using the TRIM code for calculating the penetration depth and assuming that the implanted particles come to rest at the end of the range, we get the concentration profile shown in Fig.9 for the deuterium atoms in the beam (impurities are not taken into account).

As only 75% of the beam were deuterium atoms we estimate that the concentration in a pure deuterium beam would have been 1.33 times the measured concentration, say 2.2 10^{18} $atoms/cm^2$. Using an implanted range of 0.2 - 0.6 micron (Fig.9) for 80% of the flux (impurities neglected) we get an implanted density of 4 10^{22} $atoms/cm^3$ (30 at%)

After the second charging scan, in which the surface temperature on most tiles was well above liquidus, the deuterium is released on all measured tiles apart from the uppermost three tiles, which stayed below liquidus. That the upper 3 tiles stayed below liquidus can be seen from

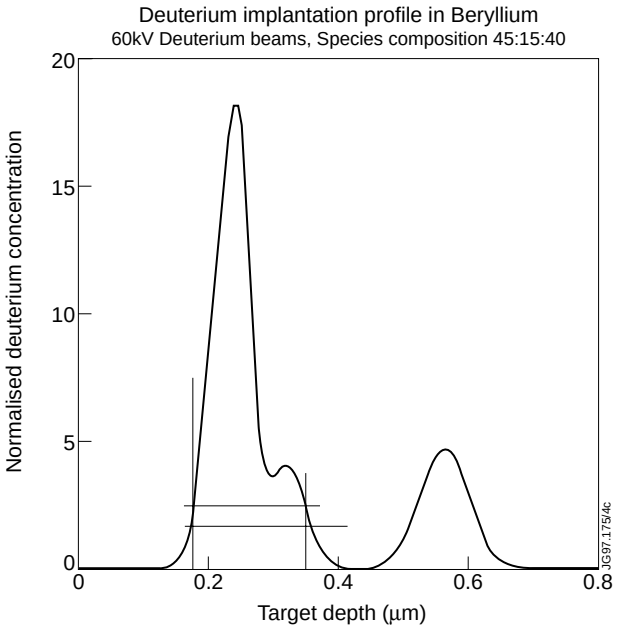

Fig.9: Deuterium deposition profile from TRIM.

Fig.10 which shows the test section **before** the first charging scan at 5 MW/m^2 (left) and **after** the second charging scan with surface melting (right). The actual surface temperature of the three unmelted tiles at the top could not be measured with the IR imaging system. If we assume that tile 3 was just below liquidus - say 1200 ^{o}C - and that the surface temperature is proportional to the thermocouple temperature we estimate a temperature of 800^{o}C for tile 1 and 1000^{o}C for tile 2.

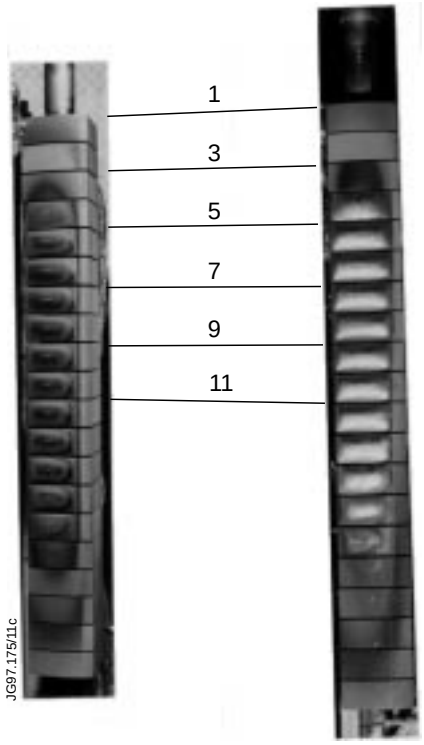

Fig.10: Photographs of the test section before the charging run at 540 K (left) and after the second charging run at high temperatures (right). No additional melting is observed on the upper three tiles.

3.2 Distribution of the implanted Deuterium

Figure 11 shows a comparison of the NRA spectrum from the center of the Monoblock (a) with a spectrum from a point on one of the Mk I Be divertor tiles after use in JET during 1995 (b). The spectrum (c) is recorded from a graphite sample implanted with $6x10^{17}$ atoms cm^{-2} of D at 5 keV, which TRIM calculations suggest should give a film 0.15 μm thick saturated with D (i.e. to a D:C ratio of 0.4:1).

The D peaks in (a) and (c) are at the same channel number (which is proportional to energy) and of the same width. Furthermore spectrum (b) shows that for a film with D present throughout the analysable depth the peak would be much wider, to higher channel numbers. (Reactions occurring at greater depth lead to protons of greater energy due to the kinematics of the reaction.) The peak from the implanted standard has a half-width perhaps a factor of ten less than from the thick (8μm or more) film, but the D is actually within 0.15 μm, so this peak width represents the resolution of the detector. The peak from the monoblock is the same width, so we can conclude that the D is certainly all within the first micron, but we cannot say how much thinner than that the layer is.

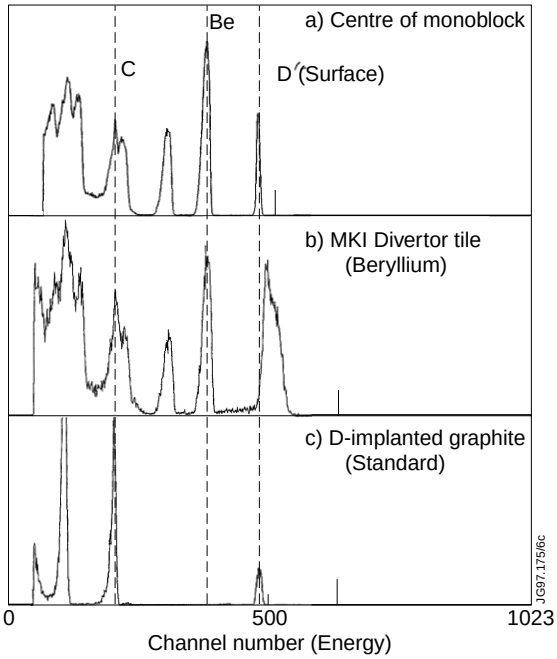

Fig.11: comparison of the NRA spectrum from the center of the Monoblock (a) with a spectrum from a point on one of the Mk I Be divertor tiles after use in JET during 1995 (b). The spectrum (c) is recorded from a graphite sample implanted with $6x10^{17}$ atoms cm^{-2} of D at 5 keV, which TRIM calculations suggest should give a film 0.15 μm thick saturated with D (i.e. to a D:C ratio of 0.4:1).

3.3 Implantation on the disc holder assembly.

After the first exposure with surface temperatures of 500 - 550 K we find an average Beryllium layer of 3 10^{16} atoms / cm^2 corresponding to a depth of 3 10^{-3} μm. The Deuterium/Beryllium

ratio is rather high but this might be wrong because of the contribution from the base material. After the second exposure the Beryllium deposit is up by two order of magnitude to 5 10^{18} atoms/cm^2 corresponding to 0.4 μm. The beam fluence in both experiments was almost the same and the thicker layer must be a consequence of the much higher evaporation rate in the second exposure. The Deuterium content increased roughly by a factor of 6 and the Deuterium Beryllium ratio is now only 3 - 4 %.

Table 3:Deposition and implantation on the disc holder assembly in atoms/cm^2

	First exposure (520K)			
Position	**C**	**BE**	**D**	**D/BE**
upper disc cover	8E+16	3E+16	3E+15	9%
upper disc	4E+16	4E++16	3E+16	74%
middle glass	3E+16	5E+16	3E+16	57%
middle glass cover	7E+16	4E+16	3E+16	61%
copper base	3E+16	5E++16	3E+16	60%
lower disc	3E+16	4E+16	3E+16	76%
lower disc cover	7E+16	3E+16	1E+16	34%
	Second exposure (>2000K)			
	C	**BE**	**D**	**D/BE**
upper disc	1E+18	4E+18	1E+17	3%
middle glass	1E+18	5E+18	2E+17	3%
middle glass cover	1E+18	5E+18	2E+17	4%
lower disc	9E+17	4E+18	2E+17	4%
lower disc cover	5E+17	4E+18	1E+17	4%

4. DISCUSSION

Our results agree perfectly well with previous measurements carried out by Moeller on Beryllium supplied by JET (S65) [6]. Fig.12 shows a summary of these results together with the

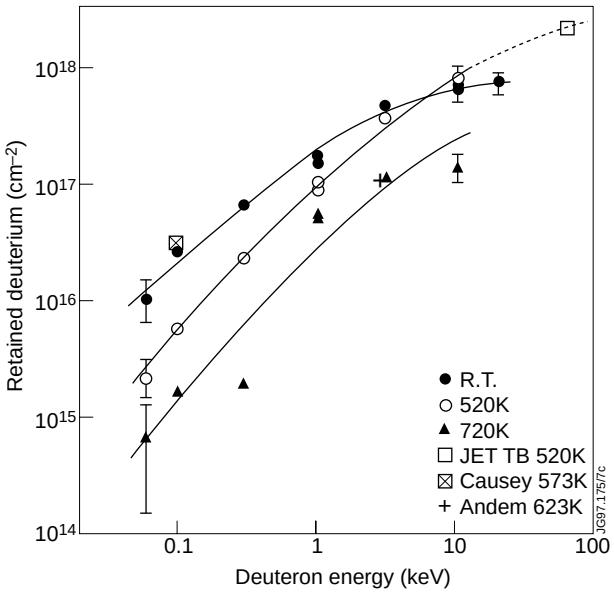

Fig.12: Comparison of the retained Deuterium in various experiments.

concentration from our first charging scan. More recent retention measurements in Beryllium with lower particle fluxes and lower energy largely agree with our results if we use the scaling of Fig.12.

1. Yoshida observes a retention of 10^{17}/cm^2 after implantation at 673 ^{o}K with 8 keV D_3^+ ions [7]. This is 5% of the implantation we find. The particle energy is roughly 10% of our energy and the particle flux is with 3 10^{14} atoms/cm^2 roughly 1% of our flux. The data point is added in Fig.12.
2. Causey [8] finds in a 100 eV plasma exposure a retention of 3 10^{16}/cm^2 at a temperature of 573 ^{o}K an a flux in the range of 1 - 3 10^{18} atoms/cm^2. This implantation is roughly 1% of our measurement, but the penetration depth is also much smaller.
3. Anderl [9] reports an implantation of 0.1 at% from a 3 keV D_3^+ beam with a flux of 5 10^{15} atoms/cm^2 on a target of 623 and 703 ^{o}K. The peak concentration was at a depth of 0.2 - 0.4 μm while the implantation depth is quoted as 0.016 μm. We find an implanted concentration of 30 at% if we believe in the deposition profile derived from TRIM.

The hydrogen density trapped in Beryllium is very high, but as the range over which hydrogen is trapped is very narrow, the total quantity of trapped hydrogen is modest, provided the hydrogen does not spread with time and fluence. Experiments to measure the spreading of the trapped hydrogen are in preparation.

The Deuterium/Beryllium ratio on the disc holder is with 3 - 4 % one order of magnitude lower than that reported by Mayer [10] in an experiment where the Beryllium and Deuterium on the target plate originate from the sputtering/reflection of a 4.5 keV D_3^+ beam on Beryllium. In our case the Beryllium originates from evaporation the codeposited deuterium can originate from reflected ions and neutrals, from gas collisions (the pressure is 2 - 3 10^{-3} mbar) or from interactions of the target with the beam plasma formed by collisions between beam particles and

background gas. The difference between our result and that of Mayer indicates that the quantity of codeposition is likely to depend on both fluxes - hydrogen and beryllium. More experiments are required to meaure the influence of energy, temperature and flux ratio.

We also conclude, that in the case of Beryllium an almost identical hydrogen retention is found in experiments with low and high fluxes. This gives confidence that the measurement is not sensitive to flux and energy.

REFERENCES

[1] H D Falter, E Thompson, D Ciric, HPL de Esch, Implantation and desorption of tritium and tritium recovery from the JET neutral beam injectors, Journal of Nuclear Materials 196-198 (1992), 1131-1134

[2] J Kim, D-D neutron and X-ray yields from high power deuterium beam injectors, Nucl. Technology 44 (1979), 315.

[3] CM Bartle, NG Chapman and PB Johnson, A study of Deuterium implantation in a copper drive in target, Nuclear Instruments and Methods (95) (1971) 221-228.

[4] B L Boyle and D K Price, Steady state hydrogen transport in solids exposed to fusion reactor plasmas, Journal of Nuclear Materials 122 & 123 (1984) 1523-1530

[5] H D Falter et al, Test Report Beryllium Monoblocks - in preparation

[6] W Moeller, B.M.U. Scherzer, and J Bohdansky, Retention and release of deuterium implanted into Beryllium, IPP-JET report No. 26, March 1985)

[7] N Yoshida, S Mizusawa, R Sakamoto, T Muroga, Radiation damage and deuterium trapping in deuterium ion injected beryllium, Journal of nuclear materials 11305 (1966)

[8] R Causey, Tritium retention in Beryllium using the Tritium Plasma Experiment, Presented at Idaho National Engineering Laboratory, Idaho Falls, ID (USA), October 14-15, 1996

[9] R A Anderl, M R Hankins, G R Longhurst, and R J Pawelko, Hydrogen transport behaviour of beryllium, Journal of nuclear materials 196-198 (1992)

[10] M. Mayer, R Behrisch, H. Plank, J. Roth, G Dollinger, and C.M. Frey, Codeposition of hydrogen with Be, C, and W. J. Nucl. Mat.

Pulse Number	Notes	Beam Voltage [kV]		Extracted power [MW]	Peak PD [MW/m²]	Peak PD [MW/m²]	Perveance [uperv]	Beam On Time [s]		MAX TC	average	Cumulativ On time	measured	flux	cumm.
		set	measured					set	measured	TEMP	flux		ratio	deut.	flux
	ITER Be monoblock – 2nd test 02–Aug–96									[°C]	[cm-2]		D/(H+D)	CM-2	D2/cm²
					Water Cal	Inertial Cal									
FORMULAS				0.00											
88864		54	55.00	0.14	0.00	0.00	0.198	1.041	0.330		0.00E+00	0.330	2.25E-01	0.00E+00	0.00E+00
88865		54	54.70	0.14	0.00	0.00	0.192	1.041	0.820		0.00E+00	1.150	2.57E-01	0.00E+00	0.00E+00
88866		54	52.30	0.13	0.00	0.00	0.205	3.041	2.780		0.00E+00	3.930	2.86E-01	0.00E+00	0.00E+00
88867		54	55.10	0.14	0.00	0.00	0.197	3.041	3.010		0.00E+00	6.940	3.37E-01	0.00E+00	0.00E+00
88868		54	55.20	0.16	0.00	0.00	0.218	3.041	3.000		0.00E+00	9.940	3.79E-01	0.00E+00	0.00E+00
88869		54	55.20	0.15	0.00	0.00	0.210	3.041	3.010		00.E+00	12.950		0.00E+00	0.00E+00
88870		54	55.20	0.15	0.00	0.00	0.210	3.041	3.010		0.00E+00	15.960		0.00E+00	0.00E+00
88871		54	55.00	0.15	7.28	6.80	0.213	3.041	3.010	116	3.23E+17	18.970		1.56E+17	1.56E+17
88872		54	55.00	0.15	7.28	6.80	0.211	3.041	3.010		3.23E+17	21.980		1.57E+17	3.13E+17
88873		54	55.00	0.15	7.28	6.80	0.211	3.041	3.010		3.23E+17	24.990		1.59E+17	4.72E+17
88874		54	55.00	0.15	7.28	6.80	0.211	3.041	3.010		3.23E+17	28.000		1.60E+17	6.32E+17
88875		54	55.00	0.16	7.28	6.80	0.215	3.041	3.010		3.23E+17	31.010		1.62E+17	7.94E+17
88876		54	55.00	0.16	7.28	6.80	0.215	3.041	3.010		3.23E+17	34.020		1.63E+17	9.57E+17
88877		54	55.00	0.15	7.28	6.80	0.212	3.041	3.010		3.23E+17	37.030		1.65E+17	1.12E+18
88878		54	54.40	0.16	5.64	6.60	0.224	6.041	6.000	156	4.99E+17	43.030	5.19E-01	2.58E+17	1.38E+18
88879		54	54.40	0.16	5.64	6.60	0.221	6.041	6.000		4.99E+17	49.030	5.11E-01	2.63E+17	1.64E+18
88880		54		0.00	5.64	6.60		6.041	6.000		4.99E+17	55.030	5.30E-01	2.67E+17	1.91E+18
88881		54		0.00	5.64	6.60		6.041	6.000		4.99E+17	61.030	5.40E-01	2.70E+17	2.18E+18
88882		54		0.00	5.64	6.60		6.041	6.000		4.99E+17	67.030	5.63E-01	2.74E+17	2.45E+18
88883		54	54.80	0.16	5.64	6.60	0.223	6.041	6.000		4.99E+17	73.030	5.62E-01	2.78E+17	2.73E+18
88884		54	54.80	0.16	5.64	6.60	0.224	6.041	6.000		4.99E+17	79.030	5.71E-01	2.81E+17	3.01E+18
88885		54	54.80	0.16	5.83	6.43	0.224	6.041	6.000	155	5.16E+17	85.030	5.79E-01	2.94E+17	3.31E+18
88886		60	58.60	0.17	5.83	6.43	0.204	6.041	6.000		4.64E+17	91.030	5.83E-01	2.68E+17	3.57E+18
88887		60	58.50	0.17	5.83	6.43	0.205	6.041	6.000		4.64E+17	97.030	5.86E-01	2.71E+17	3.85E+18
88888		60	58.10	0.17	5.86	5.86	0.208	6.041	6.000	142	4.87E+17	103.030	5.96E-01	2.75E+17	4.12E+18
88889		60	57.60	0.17	5.30	5.86	0.209	8.041	8.000		5.63E+17	111.030	5.71E-01	3.36E+17	4.46E+18
88890	No beam G3 exc err?	60		0.00	5.30	5.86		8.041				111.030	ERR	0.00E+00	4.46E+18
88891	No beam G3 exc err?	60		0.00	5.30	5.86		8.041				111.030	ERR	0.00E+00	4.46E+18
88892		60		0.00	5.30	5.86		8.041				111.030	ERR	0.00E+00	4.46E+18
88893		60	59.70	0.18	5.09	5.38	0.201	8.041	8.000		5.41E+17	119.030	5.76E-01	3.27E+17	4.78E+18
88894	G3 again	60		0.00	5.09	5.38		8.041				119.030	ERR	0.00E+00	4.78E+18
88895		60	58.40	0.17	5.17	5.86	0.206	6.041	6.000		4.11E+17	125.030	5.95E-01	2.51E+17	5.03E+18
88896		60	58.80	0.17	5.17	5.86	0.201	6.041	6.000		4.11E+17	131.030	6.18E-01	2.53E+17	5.29E+18
88897		60	59.40	0.18	5.17	5.86	0.203	6.041	6.000		4.11E+17	137.030	6.17E-01	2.55E+17	5.45E+18
88898		60	59.30	0.18	5.17	5.86	0.203	6.041	6.000		4.11E+17	143.030	6.30E-01	2.57E+17	5.80E+18
88899		60	59.40	0.18	5.17	5.86	0.201	6.041	6.000		4.11E+17	149.030	6.31E-01	2.59E+17	6.06E+18
88900		60	59.20	0.18	5.27	5.48	0.203	6.041	6.000		4.20E+17	155.030	6.42E-01	2.66E+17	6.33E+18
88901		60	57.60	0.17	5.27	5.46	0.210	6.041	6.000		4.20E+17	161.030	6.48E-01	2.68E+17	6.59E+18
88902		60	58.60	0.18	5.27	5.46	0.207	6.041	6.000		4.20E+17	167.030	6.45E-01	2.70E+17	6.86E+18
88903		60	58.30	0.17	5.27	5.46	0.208	6.041	6.000		4.20E+17	173.030	6.42E-01	2.72E+17	7.14E+18
88904		60	57.90	0.17	5.27	5.46	0.202	6.041	6.000		4.20E+17	179.030	6.56E-01	2.74E+17	7.41E+18
88905		60	59.20	0.18	5.27	5.46	0.202	6.041	6.000		4.20E+17	185.030	6.69E-01	2.75E+17	7.69E+18
88906		60	59.10	0.17	5.27	5.46	0.202	6.041	6.000		4.20E+17	191.030	6.60E-01	2.77E+17	7.96E+18
88907		60	58.90	0.17	5.27	5.46	0.203	6.041	6.000		4.20E+17	197.030	6.65E-01	2.78E+17	8.24E+18

Pulse Number	Notes	Beam Voltage [kV]		Extracted power [MW]	Peak PD [MW/m²]	Peak PD [MW/m²]	Perveance [uperv]	Beam On Time [s]		MAX TC	average	Cumulativ On time	measured	flux	cumm.
		set	measured					set	measured	TEMP	flux		ratio	deut.	flux
	ITER Be monoblock – 2nd test 02–Aug–96									[°C]	[cm-2]		D/(H+D)	CM-2	D2/cm²
					Water Cal	Inertial Cal									
FORMULAS				0.00											
88908		60	58.70	0.17	5.27	5.46	0.203	6.041	6.000		4.20E+17	203.030	6.68E-01	2.80E+17	8.52E+18
88909		60	58.20	0.17	5.27	5.46	0.204	6.041	6.000		4.20E+17	209.030	6.60E-01	2.81E+17	8.80E+18
88910		60	58.10	0.17	4.91	5.51	0.207	6.041	6.000		3.95E+17	215.030	6.71E-01	2.66E+17	9.07E+18
88911		60	58.20	0.17	4.96	5.51	0.207	6.041	6.000		3.95E+17	221.030	6.82E-01	2.67E+17	9.33E+18
88912		60	58.20	0.17	4.96	5.51	0.206	6.041	6.000		3.95E+17	227.030	6.80E-01	2.68E+17	9.60E+18
88913		60	58.00	0.17	4.96	5.51	0.207	6.041	6.000		3.95E+17	233.030	6.85E-01	2.69E+17	9.87E+18
88914		60	58.00	0.17	4.96	5.51	0.207	6.041	6.000		3.95E+17	239.030	6.84E-01	2.70E+17	1.01E+19
88915		60	57.80	0.17	4.96	5.51	0.206	6.041	6.000		3.95E+17	245.030	6.85E-01	2.72E+17	1.04E+19
88916	g3 ex. error	60		0.00	4.96	5.51		6.041				245.030	ERR	0.00E+17	1.04E+19
88917		60	57.40	0.16	5.37	5.63	0.204	6.041	6.000	137	4.28E+17	251.030	6.59E-01	2.96E+17	1.07E+19
88918		60	57.30	0.16	5.37	5.63	0.206	6.041	6.000		4.28E+17	257.030	6.85E-01	2.97E+17	1.10E+19
88919		60	57.10	0.17	5.37	5.63	0.210	6.041	6.000		4.28E+17	263.030	6.94E-01	2.98E+17	1.13E+19
88920		60	56.80	0.16	5.37	5.63	0.208	6.041	6.000	136	4.28E+17	269.030	7.03E-01	2.99E+17	1.16E+19
88921		60	56.60	0.16	5.37	5.63	0.209	6.041	6.000		4.28E+17	275.030	6.99E-01	3.00E+17	1.19E+19
88922		60	58.00	0.17	5.37	5.63	0.207	6.041	6.000		4.28E+17	281.030	7.12E-01	3.01E+17	1.22E+19
88923		60	58.30	0.17	5.37	5.63	0.203	6.041	6.000		4.28E+17	287.030	7.08E-01	3.02E+17	1.25E+19
88924		60	58.00	0.17	5.37	5.63	0.205	6.041	6.000		4.28E+17	293.030	7.05E-01	3.03E+17	1.28E+19
88925	G3 ex error	60		0.00	5.37	5.63		6.041	6.000			293.030	ERR	0.00E+00	1.28E+19
88926		60	58.60	0.17	5.37	5.63	0.199	6.041	6.000		4.28E+17	299.030	6.95E-01	3.04E+17	1.31E+19
88927		60	58.60	0.17	5.37	5.63	0.202	6.041	6.000		4.28E+17	305.030	7.11E-01	3.04E+17	1.34E+19
88928		60	58.70	0.17	5.37	5.63	0.202	6.041	6.000		4.28E+17	311.030	7.10E-01	3.05E+17	1.37E+19
88929		60	58.60	0.17	5.37	5.63	0.202	6.041	6.000		4.28E+17	317.030	7.12E-01	3.06E+17	1.40E+19
88930	trigger IR	60	58.50	0.17	4.62	5.34	0.201	6.041	6.000	130	3.68E+17	323.030	7.19E-01	2.64E+17	1.43E+19
88931		60	58.70	0.17	4.62	5.34	0.201	6.041	6.000		3.68E+17	329.030	7.21E-01	2.65E+17	1.46E+19
88932		60	58.70	0.17	4.62	5.34	0.202	6.041	6.000		3.68E+17	335.030	7.20E-01	2.65E+17	1.48E+19
88933		60	58.40	0.17	4.62	5.34	0.203	6.041	6.000		3.68E+17	341.030	7.19E-01	2.66E+17	1.51E+19
88934		60	58.10	0.17	4.62	5.34	0.203	6.041	6.000		3.68E+17	347.030	7.38E-01	2.66E+17	1.54E+19
88935		60	58.30	0.17	4.62	5.34	0.205	6.041	6.000		3.68E+17	353.030	7.28E-01	2.67E+17	1.56E+19
88936		60	58.10	0.17	4.62	5.34	0.204	6.041	6.000		3.68E+17	359.030	7.19E-01	2.67E+17	1.59E+19
88937		60	58.40	0.17	4.62	5.34	0.201	6.041	6.000		3.68E+17	365.030	7.27E-01	2.68E+17	1.62E+19
88938		60	58.60	0.17	4.62	5.34	0.200	6.041	6.000		3.68E+17	371.030	7.30E-01	2.68E+17	1.64E+19
88939		60	58.80	0.17	4.62	5.34	0.197	6.041	6.000		3.68E+17	377.030	7.25E-01	2.69E+17	1.67E+19
88940	trigger IR	60	58.90	0.17	5.06	5.06	0.199	6.041	6.000	126	4.03E+17	383.030	7.29E-01	2.95E+17	1.70E+19
88941		60	58.90	0.17	5.06	5.06	0.201	6.041	6.000		4.03E+17	389.030	7.31E-01	2.95E+17	1.73E+19
88942		60	59.90	0.17	5.06	5.06	0.196	6.041	6.000		4.03E+17	395.030	7.31E-01	2.96E+17	1.76E+19
88943		60	59.60	0.17	5.06	5.06	0.197	6.041	6.000		4.03E+17	401.030	7.30E-01	2.96E+17	1.79E+19
88944		60	59.90	0.17	5.06	5.06	0.194	6.041	6.000		4.03E+17	407.030	7.28E-01	2.97E+17	1.82E+19
88945		60	59.80	0.17	5.06	5.06	0.196	6.041	6.000		4.03E+17	413.030	7.31E-01	2.97E+17	1.85E+19
88946		60	59.20	0.17	5.06	5.06	0.201	6.041	6.000		4.03E+17	419.030	7.42E-01	2.98E+17	1.88E+19
88947		60	59.80	0.18	5.06	5.06	0.198	6.041	6.000		4.03E+17	425.030	7.28E-01	2.98E+17	1.91E+19
88948		60	59.80	0.17	5.06	5.06	0.196	6.041	6.000		4.03E+17	431.030	7.41E-01	2.98E+17	1.94E+19
88949		60	59.80	0.17	5.06	5.06	0.106	6.041	6.000		4.03E+17	437.030	7.38E-01	2.99E+17	1.97E+19
88950	Trigger IR	60	58.70	0.17	4.93	4.89	0.203	6.041	6.000	121	3.93E+17	443.030	7.48E-01	2.92E+17	2.00E+19
											3.1E+19			2.0E+19	